

THROUGH-THE-WALL DETECTION OF STATIONARY HUMAN TARGETS USING DOPPLER RADAR

R. M. Narayanan, M. C. Shastry, P.-H. Chen, and M. Levi

The Pennsylvania State University
University Park, PA 16802, USA

Abstract—In homeland security and law enforcement situations, it is often required to remotely detect human targets obscured by walls and barriers. In particular, we are specifically interested in scenarios that involve a human whose torso is stationary. We propose a technique to detect and characterize activity associated with a stationary human in through-the-wall scenarios using a Doppler radar system. The presence of stationary humans is identified by detecting Doppler signatures resulting from breathing, and movement of the human arm and wrist. The irregular, transient, non-uniform, and non-stationary nature of human activity presents a number of challenges in extracting and classifying Doppler signatures from the signal. These are addressed using bio-mechanical human arm movement models and the empirical mode decomposition (EMD) algorithm for Doppler feature extraction. Experimental results demonstrate the effectiveness of our approach to extract Doppler signatures corresponding to human activity through walls using a 750-MHz Doppler radar system.

1. INTRODUCTION

In recent years, there has been a great deal of research directed towards the use of Doppler-radar systems for monitoring human activity. Doppler-radar was first demonstrated for remotely monitoring human activity in [1,2]. SAR imaging and range detection [3–6] do not work well to distinguish human targets from cluttered background. In general, humans seldom stay still and their activities involve considerable movement of their limbs. These movements are not always captured by ranging systems. To recognize the presence of a human in a target scene, it is desirable to look at the Doppler modulations of the reflected waveforms, as these contain information about movements

Corresponding author: R. M. Narayanan (ram@enr.psu.edu).

that are characteristic of human activity [7, 8]. Doppler detection systems have the added advantages of simple design, low sampling rates, and easy deployment. Indoor environments have minimal Doppler clutter, which is highly desirable for effective detection.

Simple systems proposed in [2, 7, 9] for the detection of human Doppler utilize time domain, frequency domain [9], and spectrogram based approaches [7, 10]. The S-method is proposed in [11] for micro-Doppler based characterization. Reassigned joint time-frequency transforms are proposed in [12] for analysis. Existing systems for human Doppler detection mostly deal with gross movement of the human torso. In this paper, we consider detection and characterization of Doppler from stationary humans, i.e., wherein the human torso is not moving. In such scenarios, it is essential to extract Doppler from breathing and transient movements of the arm. In this respect, existing approaches to human Doppler analysis are limited by the time-frequency ambiguity, and the *a priori* choice of time-frequency bases, which are characteristic of traditional time-frequency distributions.

The EMD-Hilbert spectrum (referred to hereafter as EMD-HS) algorithm is a recent development in the field of time-frequency analysis [13]. It involves adaptive decomposition of a signal into constituent time-frequency components called intrinsic mode functions (IMFs). Preliminary work on using the EMD-HS approach towards human Doppler analysis was presented in [14]. We review the EMD-HS algorithm in Section 2 and define the instantaneous frequency of a signal. The detection of transient activities is often crucial to the detection of stationary human targets in the environment. The Doppler frequencies associated with human movement can be considered to result from the movement of the torso, movement of the limbs, swinging of the limbs, expansion and contraction of the chest cavity, and the changes in the position of the limbs. Human activity can be considered as a combination of one or many of these movements, and each activity occurs over a different time scale. In the most general case, significant challenges to Doppler detection arise because there is no way of knowing about the specifics of the human activity *a priori*. In Section 3, we propose a model for human activity, and consider issues involving time-frequency analysis. Based on the reasoning presented in Section 3, the criteria we choose to decide on the time-frequency technique are — frequency resolution, ability to resolve time-frequency components of low amplitude, non-linearity of transformation and adaptive selection of time-scales. These properties are satisfied by the EMD algorithm. In Section 4, we present the results of experiments involving human Doppler.

There has been considerable work in the past in the field of remote

detection of respiration in human beings. The focus in earlier work was on cooperative human targets, with the radar operating with exact knowledge about the position of the target. These systems were designed specifically for health monitoring.

In our system, we consider the problem of detecting human arm movements for security applications, where the radar operator does not have the cooperation of the target. The novel contribution of the present paper is the detection and characterization of Doppler from stationary humans, i.e., wherein the human torso is not moving. We believe this is the first paper to apply bio-mechanical models of human movement to study transient Doppler modulations due to a stationary human. In Section 4, we show that our model for human arm movement can predict Doppler signatures reasonably well using the EMD algorithm. We present experimental results that demonstrate distinct Doppler modulations that result from different types of transient, non-repetitive human activity.

2. EMPIRICAL MODE DECOMPOSITION

2.1. Introduction to EMD-HS

The EMD-HS algorithm (also called the Hilbert Huang Transform (HHT)) was proposed in [13] for analyzing non-stationary signals originating from non-linear processes. EMD extracts intrinsic oscillatory modes defined by the time scales of oscillation, called IMFs. Such functions permit the application of the Hilbert transform and the corresponding definition of instantaneous frequency in [13]. The Hilbert transform yields the analytic version of the signal, from which, the instantaneous frequency is extracted as shown in Equations (1)–(3).

$$z(t) = x(t) + jH\{x(t)\} \quad (1a)$$

$$= x(t) + jy(t) \quad (1b)$$

$$= s(t)e^{j \int \omega(t)dt}, \quad (1c)$$

where

$$s(t) = \sqrt{(x(t))^2 + (y(t))^2}, \quad (2)$$

$$\omega(t) = \frac{d \arctan \{y(t)/x(t)\}}{dt}. \quad (3)$$

In Equation (1), $H\{\}$ denotes the Hilbert transform. The functions $s(t)$ and $\omega(t)$ are the instantaneous amplitude and instantaneous frequency of the signal, respectively.

2.2. Sifting Process

The basic step of the EMD algorithm is the sifting process which essentially extracts scales of the signal. Consider a signal with P maxima and Q minima. The sifting process starts with identifying the extrema of the signal, $x(t)$, given by the set $S_{\max}^1 = x_{\max}(t_1), x_{\max}(t_2), \dots, x_{\max}(t_j), \dots, x_{\max}(t_P)$ and $S_{\min}^1 = x_{\min}(t_1), x_{\min}(t_2), \dots, x_{\min}(t_i), \dots, x_{\min}(t_Q)$. The points of set S_{\max}^1 are interpolated to form the upper envelope of the signal, \hat{x}_{\max} . Similarly, the points of the set S_{\min}^1 are interpolated to form the minimum envelope, \hat{x}_{\min} . The average envelope, $(\hat{x}_{\max} + \hat{x}_{\min})/2$ is subtracted from the original signal $x(t)$ resulting in the first iteration of the sifting process, which is expressed as $x_j^k(t)$ where k denotes the iteration ($k = 1$ for the first iteration). The iteration on k is continued until the time-average $\langle x_j^{k+1}(t) \rangle = 0$ and the number of extrema of x_j^{k+1} is no more than one less than the number of zero-crossings. For simplicity, we will drop the term $k+1$ and write the resulting function as x_j . The first sifting process produces the first IMF, with $j = 1$. Following this, the function $x_1^r = x(t) - x_1(t)$ is created, and the sifting process is repeated, resulting in $x_2(t)$, the second IMF. The IMFs are generated until the residue $x_j^r = x(t) - \sum_{n=1}^{n=j} x_n(t)$. The functions $x_j(t)$, $j = 1, 2, \dots, N$, exhaust $x(t)$ and are nearly orthogonal to one another. Since each IMF has only one extrema between any two successive zero crossings, the frequency of the signal can be directly inferred by measuring the temporal distribution of the zero crossings of the signal. Further, the IMFs have symmetric envelopes, with the difference between the number of extrema and the number of zero crossings being no more than one. Owing to these characteristics, the IMFs are referred to as being mono-component.

Since the residue is computed by successively subtracting the sifted functions from the original signal, the EMD algorithm is data driven and adaptive. Furthermore, the performance of the EMD algorithm is sensitive to the interpolation procedure which results in an inexact estimation of the envelope. The sifting process is defined for continuous signals which means that the performance of EMD depends on the sampling rate [15]. The dependence of the EMD algorithm on these factors precludes a general, unique theoretical framework for EMD. Defining a function space for the EMD algorithm is an ill-posed problem, making it difficult to construct an analytical description of EMD. However, empirically, the EMD has been shown to be effective in extracting relevant components in a variety of applications involving non-stationary signals. Its effectiveness has been demonstrated for

processing audio signals [16], global position systems [17], gravitational waves [18], seismic signals [19], etc. While wavelet decomposition decomposes a signal into components using predefined filter banks, the EMD algorithm decomposes it into components whose modes of oscillations are adaptively decided by the nature of the signal.

In the absence of an analytical formulation, the performance of the EMD algorithm is inferred from empirical observations. One of the important properties of EMD is that it behaves like a dyadic filter for a white noise input signal. The frequency of the IMFs resulting from the decomposition of a white noise signal follows an exponential trend. The first IMF represents the fastest modes of oscillation in the signal, and with subsequent IMFs, the frequency, as measured by the number of zero crossings decays exponentially as the index of the IMF. The final IMF, always has just one zero crossing. From simulations, it was found that the number of zero crossings in an intrinsic mode function is proportional to $e^{-0.6n}$, where n is the index of the IMF. Similarly, the energy of the IMFs also reduces according to an exponential rule [20].

2.3. Hilbert Spectrum

Traditional time-frequency distributions define the frequency of a signal based on the Fourier transform. This definition has the inherent property of time-frequency uncertainty, as expressed by the lower bound on the time-bandwidth product, $\Delta_t \Delta_f \geq 1/2$. The analytic signal corresponding to each IMF is constructed using the Hilbert transform. The instantaneous frequency of this analytic signal is defined as the derivative of the instantaneous phase defined in [13]. The different IMFs resulting from the EMD algorithm are orthogonal to each other. The IMFs thus represent different time-scales of oscillations, which form a set of basis functions. This implies that there is no redundancy in the information contained in the different IMFs. Using this property, a distribution is constructed from the instantaneous frequencies of each of the IMFs. This distribution is called the Hilbert spectrum (HS). Since the instantaneous frequency of the EMD-HS approach is not defined based on the Fourier transform, the time-frequency resolution is not limited by uncertainty. In our implementation, we used a modified version of the code provided in [21].

3. MODELING DOPPLER SIGNATURES DUE TO HUMAN ACTIVITY

The Doppler modulations due to human activity vary in time according to the dynamics of human movement. Non-stationary models for Doppler due to walking human targets were proposed in [8, 14]. However, walking induces high Doppler shifts in the waveform that can be observed over short time durations. The Doppler shifts due to walking also display regular repetitive frequency modulations [14], by virtue of the regularity of human gait. The finite non-zero dimensions of the human arm and other parts of the body result in a Doppler return that consists of multiple frequency components at each time instant [14]. In this paper, we are interested in modeling Doppler signatures due to movements that are characteristic of stationary humans. We conjecture that a human whose torso is not moving can be identified from the Doppler signatures due to activity such as breathing and movements of the arm.

3.1. Modeling Human Arm Motion

A characteristic Doppler event associated with stationary human targets is the movement of the arm. Details of the motion of the arm contains information regarding the intent of humans behind the wall. It is desirable to detect and characterize Doppler signatures of human arm motion for through-the-wall monitoring applications. In this section, we present a model for Doppler due to human arm movements.

Human arm motion is composed of three components, defined by the joints driving its motion. The total movement of the arm can be described by the variable movement of the wrist, the fore-arm, and motion driven by the shoulder joint. Each of these components can be considered to be a scatterer with a one dimensional geometry moving in a plane.

3.2. A General Model for Human Arm Motion

The three components of the arm, as represented by the wrist, fore-arm and arm can each be modeled as a solid shaft exhibiting rotational motion around the corresponding joint- wrist joint, elbow joint or shoulder joint. Consider that a single tone continuous transmit waveform, $x(t)$ is incident on the human arm, given by

$$x(t) = A \exp(j\omega(t)) \quad (4)$$

With reference to Figure 1(a), the line segment OA of length l_1 represents the part of the arm between the shoulder joint and the

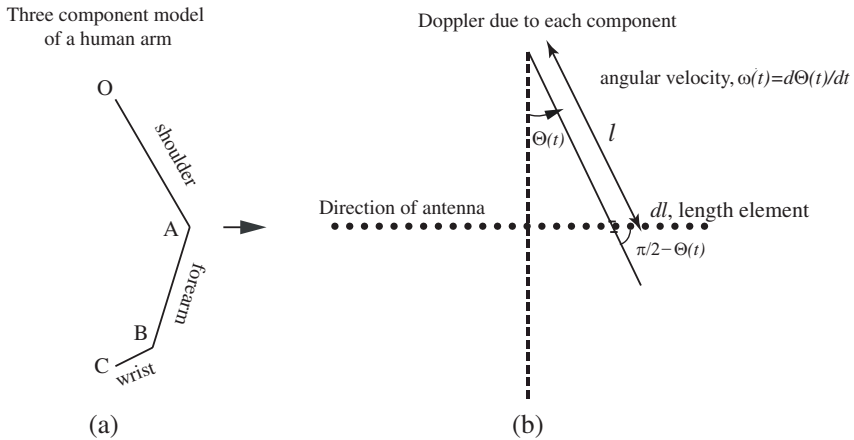


Figure 1. A schematic diagram representing the components of a human arm (a), and the Doppler due to one such component (b), that is rotating around a joint.

elbow. The line segment AB of length l_2 represents the forearm, with the point B representing the wrist joint. The line segment BC of length l_3 represents the wrist.

In such a model, the movement of the human arm is defined by the three components: ω_1 , ω_2 , and ω_3 , representing the angular velocities of the three segments OA, AB and BC, around the points defined by O, A and B, respectively. For deriving the Doppler shift resulting from this motion, we consider an infinitesimal element on each of the line segments OA, AB and BC. This element represents a point scatterer. We consider special movements, where only the i th joint flexes, while the others are fixed ($\omega_i \neq 0$, $\omega_k = 0$, $i \neq k$). Let dl represent such an element on the rotating component, at a distance l from the joint around which the rotation happens. The corresponding linear velocity along the line of sight (represented by the dotted line in Figure 1(b)) due to any of the three components is given by,

$$v_i(t) = \omega_i(t)l. \tag{5}$$

The Doppler shift is then $2v_i(t)\omega_0/c = 2\omega_i(t)l\omega_0/c$. The modulated signal resulting from the velocity of these components, can be represented as in Equation (6). The phase delay that results from

the distance to the target is ϕ .

$$s_i(t) = \int_0^{l_i} A \exp\{j(\omega_0 \pm 2((\omega_i(t)\omega_0 l/c) \cos(\theta_i(t)t))t - \phi)\} dl \quad (6a)$$

$$= \left[A \exp\{j(\omega_0 \pm 2\omega_i(t)(\omega_0/c)tl_i \cos(\theta_i(t)t) - \phi)\} \right. \\ \left. - A \exp\{j(\omega_0 t - \phi)\} \right] \frac{1}{\pm j2\omega_i(t)(\omega_0/c)t \cos(\theta_i(t)t)}. \quad (6b)$$

Thus, the return signal is a superposition of time-frequency modulations with the variation along the time axis resulting from the time-varying angular velocity. The characteristic signatures along the frequency axis, or the frequency ‘spread’ are caused due to the human arm being a continuously distributed scatterer. From Equation (6), it is clear that the length of the moving component controls this ‘spread’ in the frequency implying that a scatterer of larger dimensions results in a higher frequency-spread.

3.3. Velocity of the Human Arm

The goal of our work is to identify Doppler characteristics that distinguish human activities. This information has to be extracted from the time-dependency of the frequency, and the spread of the frequency. To that end, it is important to accurately model the time-varying velocity of a human arm. For the characteristics of the velocity of a human arm, we turn to literature in biomechanics.

3.3.1. Doppler Modeling Based on the Biomechanics of Human Movement

Doppler-radar models for human walking based on well known models of human locomotion used in computer animation are presented in [8, 22]. The effectiveness of these techniques have been demonstrated for simulating and measuring Doppler returns due to gross movement of the human body, such as walking. However, to study Doppler returns due to stationary humans, it is necessary to develop models for transient (as opposed to periodic movements such as walking) movements such as movement of a vertical, unrestrained arm in response to a stimulus. In this section, we propose a model for the motion of the human arm, primarily based on [23].

Motion of the human arm has been extensively studied. The velocity profiles for the movement of the human arm in response to different types of stimuli are presented in [24]. The objective of the paper was to understand the trajectory that the human brain plans

when responding to stimulus. The trajectory of vertical, unrestrained, human arm movement is discussed in [23]. This kind of motion is typical of stationary humans handling a large object. In such a situation, it is of interest to infer the velocity profile and trajectory that the human arm will follow in its action. The velocity of the target results in characteristic Doppler modulations of the incident waveform that are activity-specific. Consistency, in the sense that the velocity profile remaining unchanged over different subjects and trials, is important for using the features for classifying human activity.

The results in [23] and [24] suggest that a human arm moving in response to a stimulus follows a similar velocity profile across different human subjects and trials. The trajectory is defined by the joints involved in the motion. In our model, we assume the simple case of a single joint driving the human arm. In [23], the authors monitored the velocity of the human arm using a set of light emitting diodes placed on the human arm. The movement is around the shoulders with the other joints rigid. The angular velocity of the arm was found to be a unimodal function. In a single duration of arm movement,

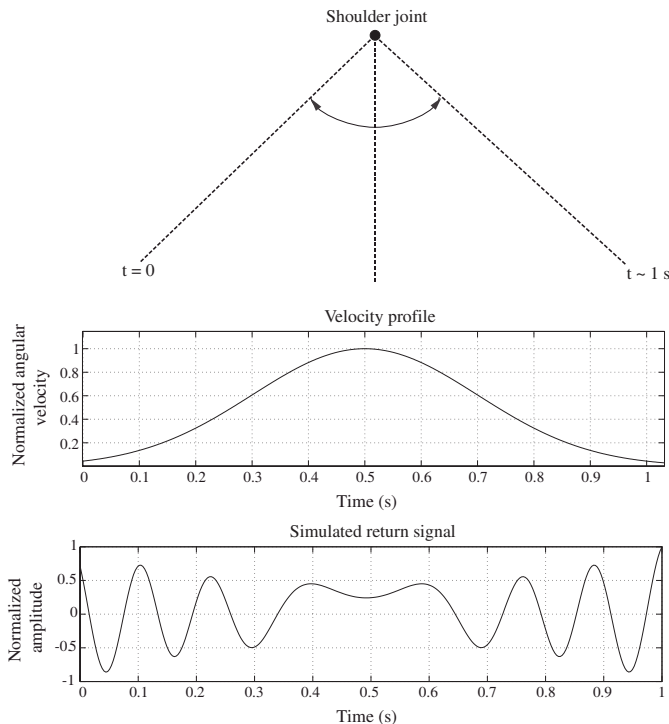


Figure 2. The velocity profile and the modeled return signal.

the velocity is continuous. The arm starts slow, the speed increases monotonically, reaches a peak at about the middle of the cycle, and reduces monotonically as it completes the task. The velocity profile is symmetric about the point of highest velocity over the duration of the response. Figure 2 shows the idealized velocity profile of human arm movement considered in [23]. The measured trajectory is given in [23]. The angular velocity, and hence the tangential velocity, can be modeled as a Gaussian function [23] of time. We can represent the velocity as:

$$\omega(t) = k_1 e^{-k_2(t-\tau)^2} \quad (7)$$

$$v_t(t) = lk_1 e^{-k_2(t-\tau)^2} \quad (8)$$

where, k_1 , k_2 , and τ are arbitrary constants that vary across different subjects and trials. Since a Gaussian velocity profile is unique to the motion of the human arm, we conjecture that it is possible to use the shape of the velocity profile would indicate with a high level of certainty the presence of a human target.

We now consider the problem of modeling the reflected signal for a single tone incident waveform, using the velocity model described above. Let the human arm be located at a distance from the receiver of a few meters. We assume it to be a one-dimensional solid scatterer with a continuous spatial distribution. We then apply the procedure of integrating the Doppler shift across the dimension of the arm. The Doppler shift due to a single element of the human arm is integrated over the entire length. We drop the subscript i from Equation (6) for convenience. We set $\theta(t) = 0$, since the variation of the angle $\theta(t)$ that the arm subtends with the vertical axis is negligible over the duration of motion. Equation (6b) then reduces to,

$$s(t) = \frac{A \exp\{j((\omega_0 \pm 2\omega(t)l/c)t - \phi)\} - A \exp\{j(\omega_0 t - \phi)\}}{\pm j2\omega(t)(\omega_0/c)t} \quad (9)$$

with the constraint that when $|t|$ is sufficiently large, $\omega(t)$ is small. The simulation results using this model are presented in Figure 2. The unimodal velocity profile over the duration of motion is seen to result in a return signal with four distinct maxima and a region of stationary points close to the time instant of maximum velocity.

3.4. Intermittent Human Activity

In the previous section, we considered a single cycle of human arm movement. Over a longer time-period of observation of time T , a human may exhibit different types of motion over different time-intervals. The return signal can then be represented as a linear

combination of different waveforms, each of which is non-zero over a different time interval and with each waveform corresponding to the Doppler modulation due to the human activity. Let $x(t)$ be the transmitted signal, and let T be the time duration over which the human target is observed. We can mark out time instances $t_0, t_1, t_2, \dots, t_n$, over the duration T , each time instant signifying a change in the movement of the human. T is then divided into time bins of length $t_1 - t_0, t_2 - t_1, \dots, t_n - t_{n-1}$, which are not necessarily equal. Over each time interval, a different type of human motion results in a different Doppler modulation of the transmit signal which is represented as a non-stationary signal $a_i(t)$. Since we are considering the case of a stationary human, the functions $a_i(t)$, denote the modulation of a sinusoid due to the different moving components of the target scene. Then, one can write the complete return signal as

$$y(t) = \sum_{i=1}^{n-1} a_i(t)(u(t - t_{i+1}) - u(t - t_i)). \quad (10)$$

The detection of human presence in a target scene can be formulated as the detection of the presence of Doppler in any of these time bins. Due to the unpredictable and irregular nature of human movement, these time-intervals are assumed to be unknown to the radar operator. Without a knowledge of t_i , it is not possible to pre-define optimum time and frequency resolutions for computing the joint time frequency distributions. The spectrogram of $y(t)$ is described as,

$$Y(t, \omega) = \int_{-\infty}^{\infty} y(t)w(t - \tau)e^{-j\omega t} dt \quad (11a)$$

$$= \int_{-\infty}^{\infty} \left(\sum_{i=1}^{n-1} a_i(t)(u(t - t_{i+1}) - u(t - t_i)) \right) w(t - \tau)e^{-j\omega t} dt. \quad (11b)$$

The drawback of using traditional time-frequency techniques for such scenarios arises from the choice of the window function $w(t)$, that needs to be optimally chosen *a priori*. If for some $a_i(t)$, the events are non-stationary within the width of the window function $w(t)$, then the spectrogram will fail to capture the complete time-frequency distribution of $a_i(t)$. In effect, the spectrogram will miss Doppler signatures due to the corresponding event. This is undesirable as it affects the reliability of the detection algorithm.

The effectiveness of the EMD algorithm is demonstrated by considering the example of radar returns from a human hand that moves intermittently for a short period of time at different instances during a 20 s interval. Two of these events occur with less than 2 s of

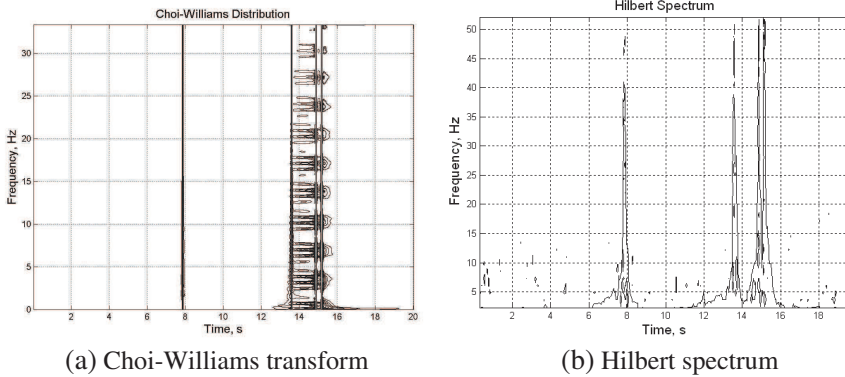


Figure 3. Comparison of conventional time-frequency representation with the Hilbert spectrum for the detection of intermittent human activity.

spacing at 13.53s and 14.88s. Time-frequency components occurring at arbitrarily close time instants are not resolved by traditional time-frequency transforms with basis functions that are defined *a priori*. An example of such a representation is the Choi-Williams transform [25]. The inherent time-frequency uncertainty and the presence of cross-terms [25] in the Choi-Williams representation distort the time-frequency spectrum. The EMD-HS algorithm, on the other hand, preserves local information due to the absence of an integrating operation in computing the frequency spectrum, as compared in Figures 3(a) and 3(b).

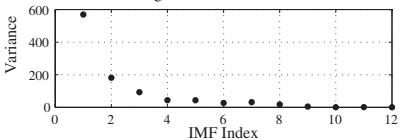
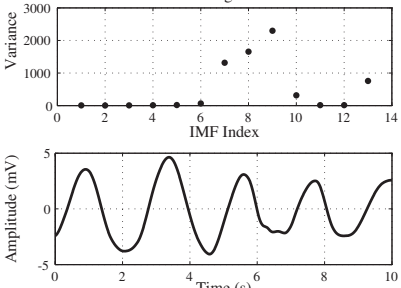
4. EXPERIMENTAL RESULTS

A human target located behind a brick wall of about 16 cm thickness was imaged using a radar system operating in the ultrahigh frequency (UHF) band. In this frequency band, the attenuation offered by the wall can be neglected. The probing waveform used for the Doppler measurements was a 750-MHz single tone waveform. The transmitted power was -5 dBm and the antenna gain was 5 dB. The Doppler detection system developed by us [26] is able to extract Doppler features from a human target in near-real time, with a latency of about 2–3 seconds for computation of the IMFs. The signal reflected from the target is down-converted to baseband by mixing with a copy of the transmit waveform. The signal is passed through a low pass filter and sampled at 50 kHz for acquisition. This sampling rate is sufficiently larger than the Nyquist rate as the bandwidth of the Doppler signatures is of the order of a few Hz. The antenna stand off from the wall was

about 1 m and the human was situated between 1 m to 2 m from the wall.

The experiment involved a human performing various controlled activities. For each activity, the Doppler return data were recorded for a time duration of 10 seconds. Significant activities relating to a stationary human involve movements of the arm and the chest cavity (due to breathing) which result in non-stationary return signals. However, the first problem to solve in the detection of the presence of humans based on Doppler signatures is to distinguish between reflected signal in the absence of a human from the case where the target scene contains an active human. The application of the EMD algorithm to characterize random noise has been discussed in [20]. In the absence of human activity, the waveform resulting from mixing the reflected signal with the transmitted signal will not consist of any Doppler components. We use the EMD to characterize the absence of a human target by noting the energy distribution across the IMFs. An exponential decay in the energy from the higher frequency IMF down to the lower frequency IMF indicates that that the signal does not contain any Doppler features. This result is shown in the first row of Table 1.

Table 1. Summary of the Doppler signatures generally associated with transient and irregular activity. The signatures show the different time-scales over which the events occur.

Target description	Energy Distribution across and Reconstructed Doppler Signatures
Absence of human in the target scene.	<p style="text-align: center;">Target scene without human</p> 
Human standing still and breathing.	<p style="text-align: center;">Breathing human</p> 

Target description	Energy Distribution across and Reconstructed Doppler Signatures
<p>Human repeatedly shuffling in a seated position.</p>	<p style="text-align: center;">Shuffling in a seated position</p>
<p>Human moving arms repeatedly in an up-and-down movement in a rapid manner.</p>	<p style="text-align: center;">Rapid arm movement</p>
<p>Human shifting position by moving for about 2 s while standing.</p>	<p style="text-align: center;">Shifting position while standing</p>
<p>Human lifting a large object off the ground over a duration of about 7 seconds.</p>	<p style="text-align: center;">Lifting an object off the ground</p>

The 750-MHz radar system was used to extract Doppler signatures associated with different activity associated with a stationary human. The general approach was to observe the energy content of each scale of oscillations of the IMFs. This is plotted as the energy of the IMFs against the index of the IMF in Table 1. The IMFs are indexed inversely as the scales of oscillations. The highest oscillation scale is associated with the first IMF and so on. For each signal, the six highest energy IMFs are added to extract the Doppler modulations.

It is to be observed that for each of the activity described in Table 1, the approximate center frequency (proportional to the transmit frequency of 750 MHz) of the Doppler features is of the order of 1–2 Hz. Such low frequencies imply that there are too few cycles to integrate for accurate representation with time-frequency transforms. For instance, the Doppler oscillation caused by a person shuffling from a stationary position for about 2 s produces features of about 1.5 Hz that last over a short time duration of 2 s. Of special interest to applications in homeland security and earthquake survivor detection is the detection of breathing. In our experiments, we found that slow and consistently periodic oscillations, of a period of about 3 seconds are characteristic of human breathing. This center frequency of the Doppler features, of about 0.3 Hz corresponds to a velocity of a few cm/s, which is the approximate velocity of a chest cavity in a person who is breathing heavily. The scales of oscillations can possibly be used to assess the intent of the human target being imaged. Doppler signatures of a human striking a victim or reaching down to lift an object off the ground are shown in Table 1. These are seen to be different from the deterministic features resulting from the motion of a human arm reaching for an object in a vertical motion around the shoulder that are described in subsequent sections. Similarly, Table 1 shows how Doppler features due to a breathing human are significantly different from a human shuffling in a seated position.

4.1. Signatures of Different Types of Arm Movement

We now consider the special case of the motion of different components of a human arm. The human arm model was earlier described as consisting of three components, centered at the shoulder, the elbow and the wrist joints. Figure 4 illustrates Doppler features extracted from the two experiments. In the first experiment, the human target repeatedly moved the wrist around the wrist joint for a duration of 10 seconds, while keeping the rest of the arm stationary. The energy distribution across the IMFs is considerably flat, and demonstrates that the energy is concentrated within a small number of IMFs. The second experiment involved the human moving the whole arm around

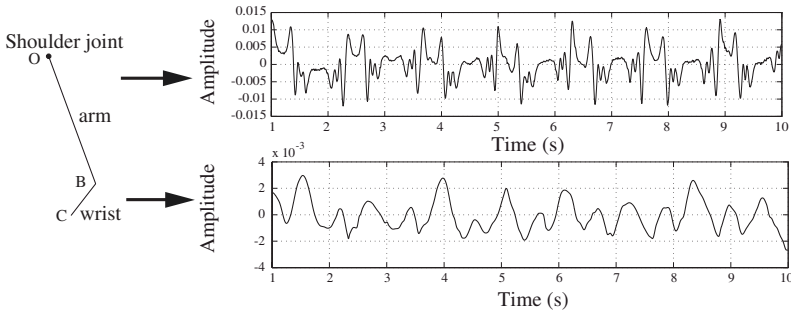


Figure 4. A comparison of the Doppler signatures resulting from movement of the wrist (bottom) and movement of the whole arm (top).

the shoulders, without any motion around the elbow and the wrist joints. The number of non-stationary oscillatory components in the former is higher than in the latter. This observation conforms to the model described in Section 3, showing the dependence of the number of significant oscillatory modes on the length of the moving scatterer.

4.2. Experimental Verification of the Kinematic Model

In this section, we present the experimental results of human arm movement. A human situated about 1.5 m from the antenna was moving one arm as if in response to a stimulus. The return waveform was processed as described earlier. The signal was decomposed using EMD and the most significant IMFs were added to reconstruct the Doppler signal. The resulting plots for three different trials with different subjects are shown in Figure 5.

The Doppler signatures acquired in the experiments of Figure 5 are seen to be just as predicted by the model described in Section 3, and Figure 2. The dashed line in Figure 5 represents the modeled waveform, and the solid line, the experimental result. The shape of the curve consistently remains the same across different trials, and corresponds closely to the model each time. This demonstrates the viability of characterizing activities associated with a stationary human using a model based approach. The experimental results validated the theoretical results as given by the Gaussian velocity profile model even when different individuals were used as targets. This invariance means that the human arm movement model described in this paper is a good candidate as a pattern to indicate the presence of human targets behind barriers. The velocity profile also provides the radar operator with valuable information about the nature of human activity in the absence of regular gross movement such as walking.

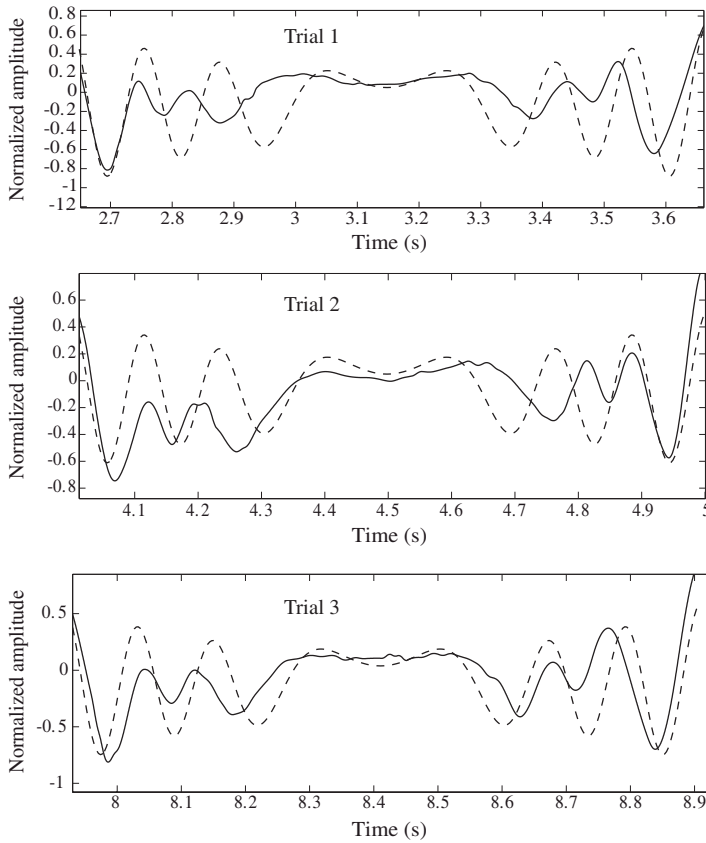


Figure 5. Plot of the return signal from a moving human arm for a number of trials. The solid line shows the experimental results and the dashed line is the modeled result.

5. CONCLUSION

We have developed a system for through-the-wall detection of a stationary human, based on the empirical mode decomposition-Hilbert spectrum algorithm. The Doppler detection system was validated by testing the algorithm on real data. The EMD algorithm was applied to extract Doppler characteristics resulting from various activities associated with a human whose torso is nearly stationary. A bio-mechanical model was developed to model a moving human arm as a radar target. The modeled waveform compared favorably with experimental results. A model based approach for classifying human activity was thus shown to be feasible.

Doppler modulations due to different types of human activity were shown to occur over different scales. As a result, we believe that it is possible to use statistical measures to classify these signals as arising from different activities. With a sufficiently large number of realizations of these experiments, it is possible to train statistical models to automatically classify Doppler signatures from transient, arbitrary human activity. Such a system for the automatic recognition of human activity associated with a stationary human is a topic of current research.

ACKNOWLEDGMENT

This research was supported by Air Force Office of Scientific Research (AFOSR)/Air Force Research Laboratory (AFRL) contract number FA9550-07-C-0066 through Intelligent Automation, Inc. The authors would like to express their gratitude to Dr. Arje Nachman of AFOSR and Dr. Richard Albanese of AFRL for valuable comments and suggestions.

REFERENCES

1. Greneker, E. F., "Radar sensing of heartbeat and respiration at a distance with security applications," *Proc. SPIE Conf. Radar Sensor Technol. II*, Vol. 3066, 22–27, Orlando, FL, April 1997.
2. Greneker, E. F., "Radar flashlight for through-the-wall detection of humans," *Proc. SPIE Conf. Targets Backgr.: Charact. Represent. IV*, Vol. 3375, 280–285, Orlando, FL, April 1998.
3. Ahmad, F., G. J. Frazer, S. A. Kassam, and M. G. Amin, "Design and implementation of near field wideband synthetic aperture beamformer," *IEEE Trans. Aerosp. Electron. Syst.*, Vol. 40, No. 1, 206–220, 2004.
4. Franceschetti, G., J. Tatoian, D. Giri, and G. Gibbs, "Timed arrays and their application to impulse SAR for through-the-wall imaging," *IEEE Antennas Propag. Soc. Int. Symp. Dig.*, 3067–3070, Monterey, CA, June 2004.
5. Nag, S., M. A. Barnes, T. Payment, and G. Holladay, "Ultrawideband through-wall radar for detecting the motion of people in real time," *Proc. SPIE Conf. Radar Sens. Technol. Data Vis.*, Vol. 4744, 48–57, Orlando, FL, April 2002.
6. Attiya, A. M., A. M. Bayram, A. Safaai-Jazi, and S. M. Raid, "UWB applications for through wall detection," *IEEE Antennas*

- Propag. Soc. Int. Symp. Dig.*, 3079–3082, Monterey, CA, June 2004.
7. Geisheimer, J. E., E. F. Greneker, and W. S. Marshall, “High-resolution Doppler model of the human gait,” *Proc. SPIE Conf. Radar Sens. Technol. Data Vis.*, Vol. 4744, 8–18, Orlando, FL, April 2002.
 8. Van Dorp, P. and F. C. A. Groen, “Human walking estimation with radar,” *IEE Proc. Radar Sonar Navig.*, Vol. 150, No. 5, 356–365, 2003.
 9. Falconer, D. G., R. W. Ficklin, and K. G. Konolige, “Robot-mounted through-wall radar for detecting, locating, and identifying building occupants,” *Proc. IEEE Int. Conf. Robot. Autom.*, 1868–1875, San Francisco, CA, July 2000.
 10. Kim, Y. and H. Ling, “Human activity classification based on micro-Doppler signatures using a support vector machine,” *IEEE Trans. Geosci. Remote Sens.*, Vol. 47, No. 5, 1328–1337, 2009.
 11. Thayaparan, T., S. Abrol, E. Riseborough, D. Stankovic, L. Lamothe, and G. Duff, “Analysis of radar micro-Doppler signatures from experimental helicopter and human data,” *IEE Proc. Radar, Sonar Navig.*, Vol. 1, No. 4, 289–299, 2003.
 12. Ram, S. S., Y. Li, A. Lin, and H. Ling, “Doppler-based detection and tracking of humans in indoor environments,” *J. Franklin Inst.*, Vol. 345, No. 6, 679–699, 2008.
 13. Huang, N. E., Z. Shen, S. R. Long, M. C. Wu, H. H. Shih, Q. Zheng, N. C. Yen, C. C. Tung, and H. H. Liu, “The empirical mode decomposition and the Hilbert spectrum for nonlinear and non-stationary time series analysis,” *Proc. R. Soc. A*, Vol. 454, No. 1971, 679–699, 1998.
 14. Lai, C.-P., R. M. Narayanan, Q. Ruan, and A. Davydov, “Hilbert-Huang transform analysis of human activities using through-wall noise and noise-like radar,” *IET Radar Sonar Navig.*, Vol. 2, No. 4, 244–255, 2008.
 15. Rilling, G. and P. Flandrin, “On the influence of sampling on the empirical mode decomposition,” *Proc. Int. Conf. Acoust. Speech Signal Process.*, Vol. 3, 444–447, Toulouse, France, May 2006.
 16. Heydarian, M. and J. D. Reiss, “Extraction of long-term structures in musical signals using the empirical mode decomposition,” *Proc. 8th Int. Conf. on Digit. Audio Eff.*, 258–261, Madrid, Spain, September 2005.
 17. Kamath, V., Y.-C. Lai, L. Zhu, and S. Urval, “Empirical mode decomposition and blind source separation methods for

- antijamming with GPS signals,” *IEEE/ION Position Location Navig. Symp.*, Vol. 1, 335–341, San Diego, CA, April 2006.
18. Camp, J. B., J. K. Cannizzo, and K. Numata, “Application of the Hilbert-Huang transform to the search for gravitational waves,” *Phys. Rev. D*, Vol. 75, No. 6, 061101.1–5, 2007.
 19. Zhang, R. R., S. Ma, and S. Hartzell, “Signatures of the seismic source in EMD-based characterization of the 1994 Northridge, California earthquake recordings,” *Bull. Seismol. Soc. Am.*, Vol. 93, No. 1, 501–518, 2003.
 20. Flandrin, P., G. Rilling, and P. Goncalves, “Empirical mode decomposition as a filter bank,” *IEEE Signal Process. Lett.*, Vol. 11, No. 2, 112–114, 2004.
 21. Rilling, G. and P. Goncalves, *EMD Toolbox for MATLAB*, <http://perso.ens-lyon.fr/patrick.flandrin/emd.html>, 2008.
 22. Ram, S. S. and H. Ling, “Micro-Doppler signature simulation of computer animated human and animal motions,” *IEEE Antennas Propag. Soc. Int. Symp. Dig.*, 679–699, San Diego, CA, July 2008.
 23. Atkeson, C. and J. Hollerbach, “Kinematic features of unrestrained vertical arm movements,” *J. Neurosci.*, Vol. 5, No. 1, 2318–2330, 1985.
 24. Hollerbach, J. and T. Flash, “Dynamic interactions between limb segments during planar arm movement,” *Biol. Cybern.*, Vol. 44, No. 1, 67–77, 1983.
 25. Choi, H. and W. J. Williams, “Improved time-frequency representation of multicomponent signals using exponential kernels,” *IEEE Trans. Acoust. Speech Signal Process.*, Vol. 37, No. 6, 862–871, 1989.
 26. Chen, P.-H., R. M. Narayanan, C. P. Lai, and A. Davydov, “Through wall ranging and imaging using UWB random noise waveform: System design considerations and preliminary experimental results,” *IEEE Antennas Propag. Soc. Int. Symp. Dig.*, doi: 10.1109/APS.2009.5172369, Charleston, SC, June 2009.